Electronic Supplementary Material (ESI) for Journal of Materials Chemistry A.
This journal is © The Royal Society of Chemistry 2023

Electronic Supplementary Information

Multifunctional Mg_2Si monolayer with negative Poisson's ratio and ultrahigh thermoelectric performance at room temperature

Xin Yu[a], Wenyuan Jin[a,b], Jiafei Pang[a], Jingning Zuo[c], Xiaoyu Kuang[*a] and Cheng Lu[*c]

[a]*Institute of Atomic and Molecular Physics, Sichuan University, Chengdu 610065, China*

[b]*Institute of Physics, Henan Academy of Sciences, Zhengzhou 450046, China*

[c]*School of Mathematics and Physics, China University of Geosciences (Wuhan), Wuhan 430074, China*

[*]*E-mails: scu_kuang@163.com; lucheng@calypso.cn*

Computational Methods During the process of searching the ground state of Mg_2Si monolayer by CALYPSO package, we considere the stoichiometric of 2:1. The initial structures are randomly generated through plane group symmetry operations and then relaxed. We select 60% of the low-energy structures to produce next generation. Finally, after 30 generations, over 1500 planar and folded Mg_2Si monolayer structures are obtained. We select and optimize the top 10 low-energy structures to find the true ground state structure. It is found that the Mg_2Si monolayer proposed in this work is the most stable by stability calculation.

The in-plane Young's modulus ($E(\theta)$) and Poisson's ratio ($\nu(\theta)$) with directional dependence can be calculated based on the theory of elastic solids,[1] as follows:

$$E(\theta) = \frac{C_{11}C_{22} - {C_{12}}^2}{C_{11}\sin^4\theta + C_{22}\cos^4\theta + A\sin^2\theta\cos^2\theta} \tag{1}$$

$$\nu(\theta) = -\frac{B\sin^2\theta\cos^2\theta - C_{12}(\sin^4\theta\cos^4\theta)}{C_{11}\sin^4\theta + C_{22}\cos^4\theta + A\sin^2\theta\cos^2\theta} \tag{2}$$

where C_{ij} is the elastic constant, θ is the angle, $A = (C_{11}C_{22} - {C_{12}}^2)/C_{66} - 2C_{12}$ and $B = C_{11} + C_{22} - (C_{11}C_{22} - {C_{12}}^2)/C_{66}$.

The cohesive energy of Mg_2Si monolayer can be calculated by the following equation:

$$E_{coh} = \frac{mE_{Mg} + nE_{Si} - E_{Mg_2Si}}{m+n} \tag{3}$$

where E_{Mg} and E_{Si} are the energies of the Mg atom and the Si atom, respectively. E_{Mg_2Si} is the total energy of the Mg_2Si monolayer. The m and n represent the number of Mg and Si atoms in the primary cell, respectively.

The lattice thermal conductivity of Mg_2Si monolayer using Cahill–Watson–Pohl (CWP) model (κ_{cwp}) is calculated by the following equation:[2]

$$\kappa_{cwp} = (\frac{\pi}{6})^{1/3}k_B n^{2/3}\sum_i v_i(\frac{T}{\theta_i})^2\int_0^{\theta_i/T}\frac{x^3e^x}{(e^x-1)^2}dx \tag{4}$$

where k_B, n, v_i, and θ_i are Boltzmann constant, atom density, the phonon velocity and Debye

temperature of the acoustic branch i, respectively. The Debye temperature is $\theta_i = v_i(\frac{\hbar}{k_B})(6\pi^2 n)^{1/3}$.

The carrier mobility of 2D materials can be calculated by[3]

$$\mu_{2D} = \frac{e\hbar^3 C_{2D}}{k_B T m^* m_d{}^* E_1{}^2} \tag{5}$$

where e, C_{2D}, k_B, m^*, $m_d{}^*$, E_1 are electron charge, elastic constant, Boltzmann constant, effective mass, average effective mass and deformation potential constant, respectively. The C_{2D} can be calculated by $C_{2D} = [\partial^2 E/\partial(\Delta a/a_0)^2]/S_0$, where E, a_0, Δa, and S_0 are the total energy of the system under strain, lattice parameters, the change value of lattice parameters, and the area of unstrained unit cell after structure optimization, respectively. m^* can be obtained from $m^* = \hbar^2/(\partial^2 E/\partial k^2)$, and $m_d{}^* = \sqrt{m_x{}^* m_y{}^*}$. The E_1 can be obtained by $E_1 = \partial E_{edge}/\partial E(\Delta a/a_0)$, where E_{edge} is the band-edge energy of Mg_2Si monolayer. Therefore, we can get the τ from carrier mobility as follows

$$\tau = \frac{\mu m^*}{e} \tag{6}$$

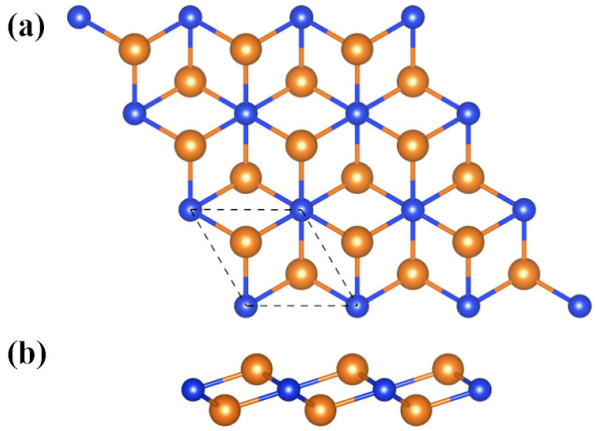

Fig. S1 The (a) top and (b) side views of T-phase Mg_2Si monolayer crystal structure. The blue balls represent Si atoms and the orange balls represent Mg atoms.

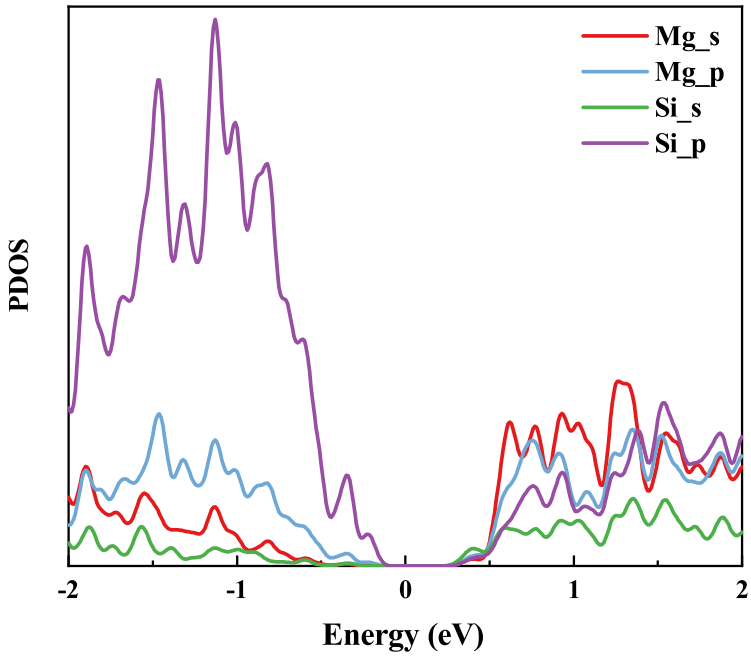

Fig. S2 Projected density of states of Mg_2Si monolayer.

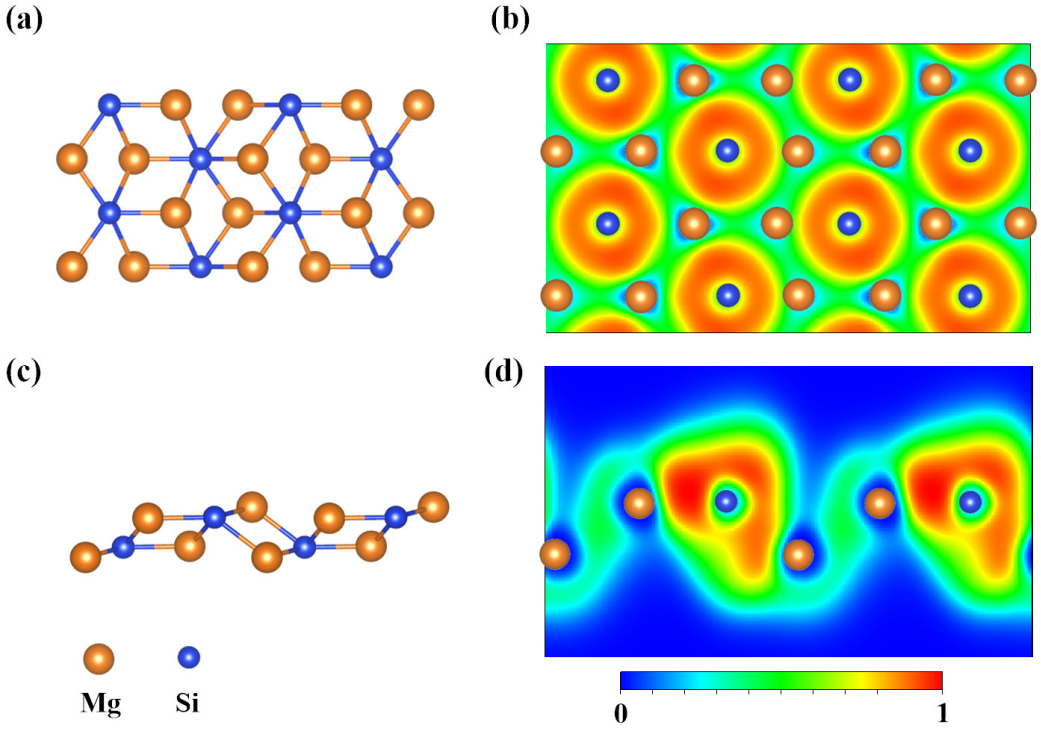

Fig. S3 (a) Top and (c) side views of two-dimensional Mg_2Si. Electronic localization function of (b) top and (d) side views of Mg_2Si monolayer.

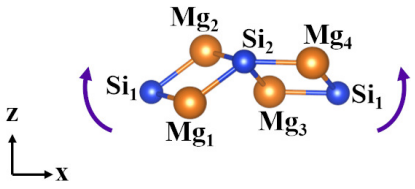

Fig. S4 Variation of Mg_2Si monolayer structure under stretch strain along x direction.

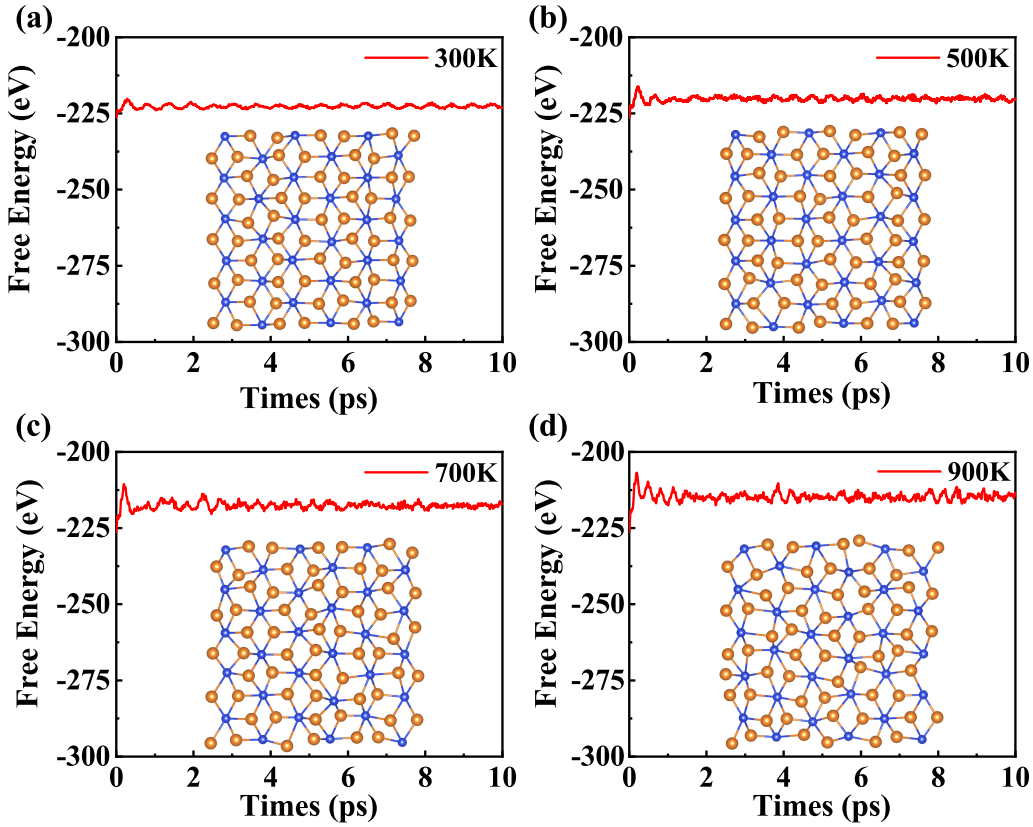

Fig. S5 The fluctuation of free energy of two-dimensional Mg_2Si monolayer (a-d) at 300-900 K is achieved by AIMD simulations lasting 10 ps. The inset of figures show the crystal structures of Mg_2Si monolayer at different temperatures. The curves of free energy at different temperatures do not fluctuate widely after 1 ps, providing sufficient evidence for its thermal stability. More computational resources will be required when the longer simulation time is used. The simulation time of 10 ps not only ensures the accuracy of calculation, but also considers the utilization of computational resources. And in many other two-dimensional materials,[4,5] the thermal stability of the materials are also calculated by using molecular dynamis simulations lasting 10 ps. Therefore, simulation time of 10 ps is enough to determine the thermal stability of Mg_2Si monolayer.

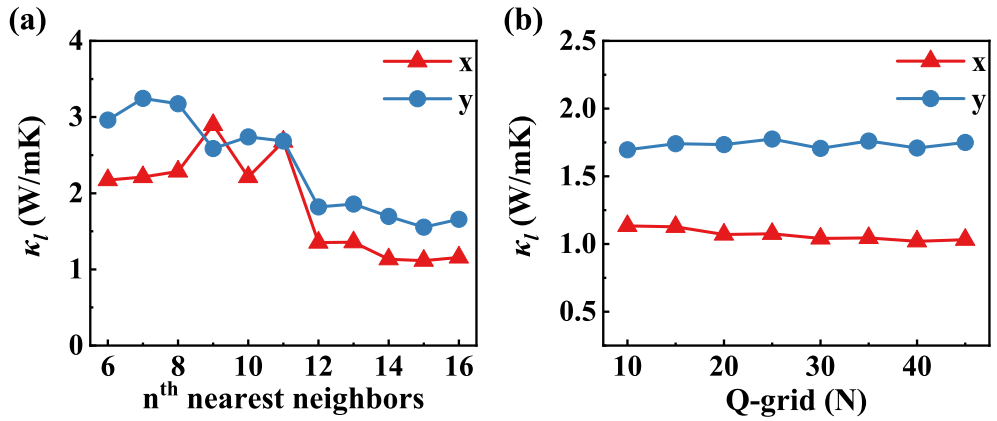

Fig. S6 Convergence test of the lattice thermal conductivity of Mg_2Si monolayer with the change of (a) nearest neighbors and (b) Q-grid.

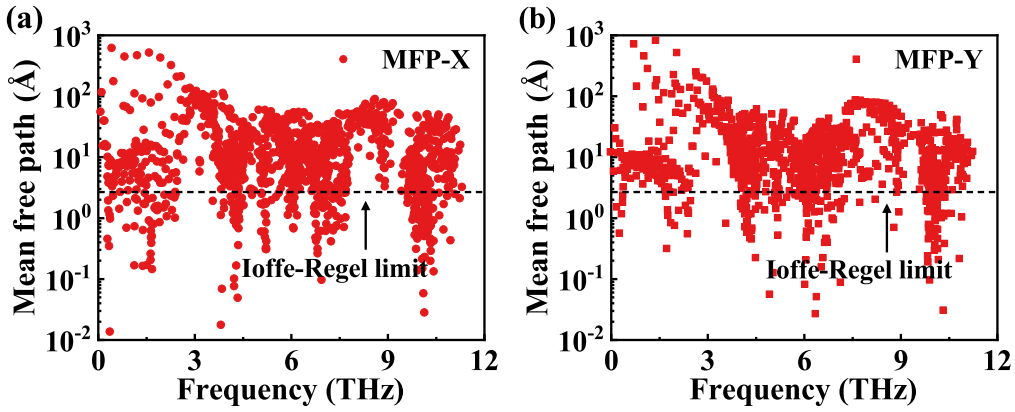

Fig. S7 The (a, b) phonon mean free path of Mg_2Si monolayer as functions of the frequency at 300 K.

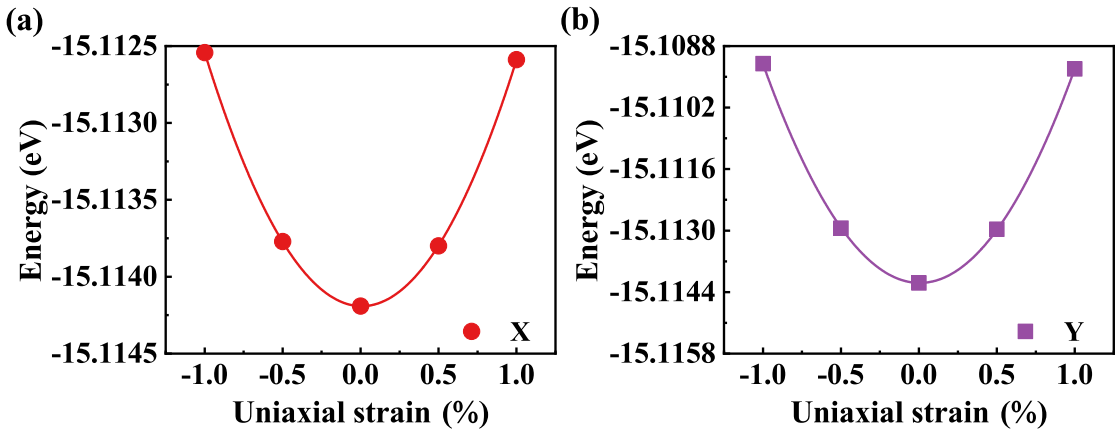

Fig. S8 The total energy of Mg_2Si monolayer under different strain with respect to the strain along (a) *x* and (b) *y* directions.

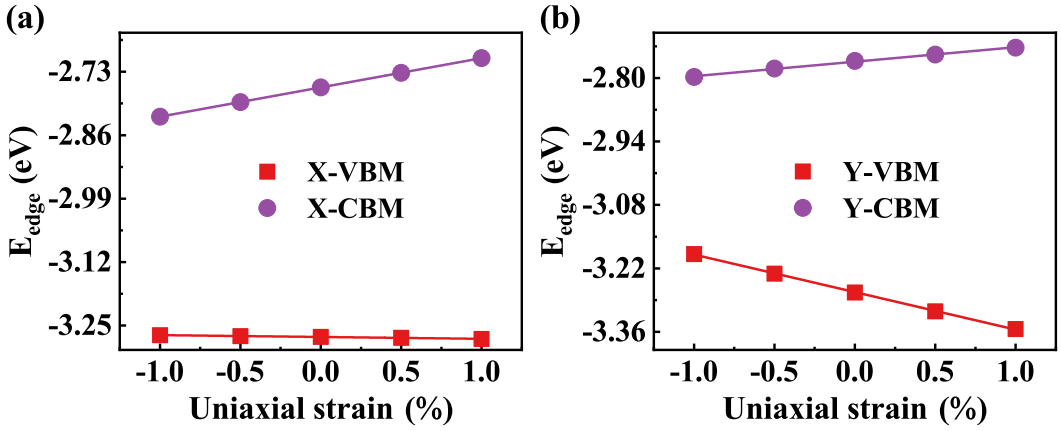

Fig. S9 The edge energies shift of VBM and CBM of Mg_2Si monolayer with respect to the strain along (a) *x* and (b) *y* directions.

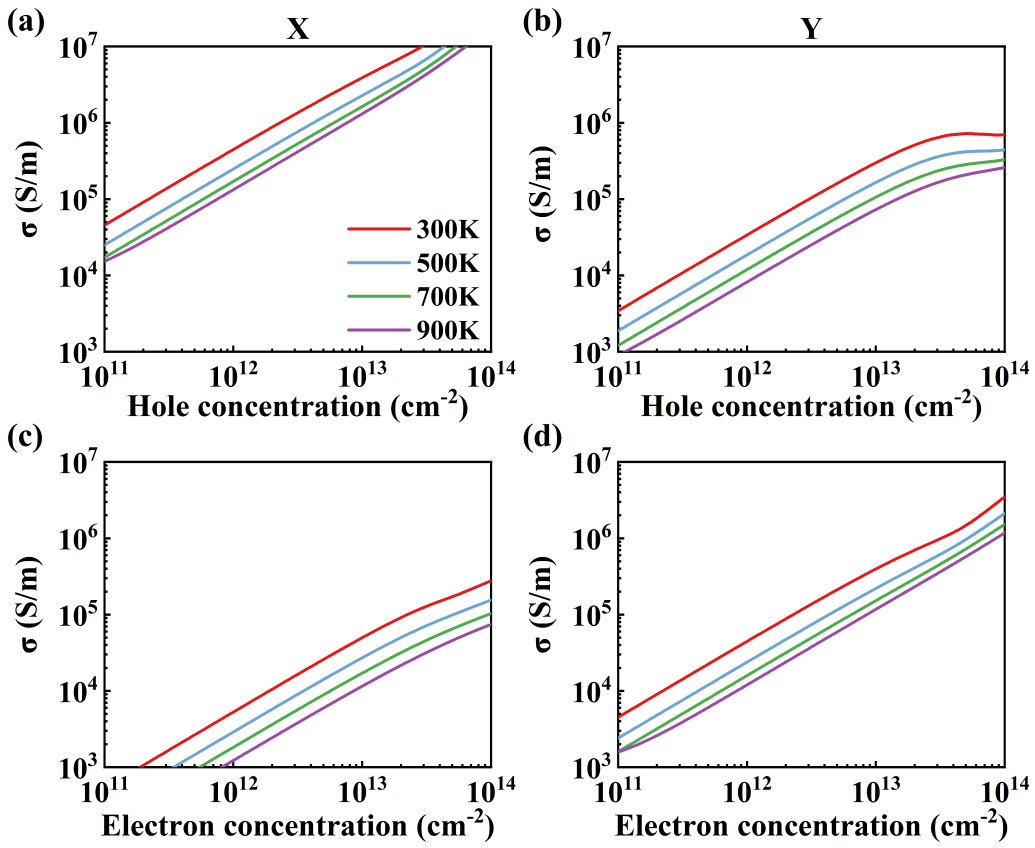

Fig. S10 The electrical conductivity of the Mg_2Si monolayer as the function of (a, b) hole or (c, d) electron doping concentration along *x* or *y* direction at different temperatures at HSE06 method.

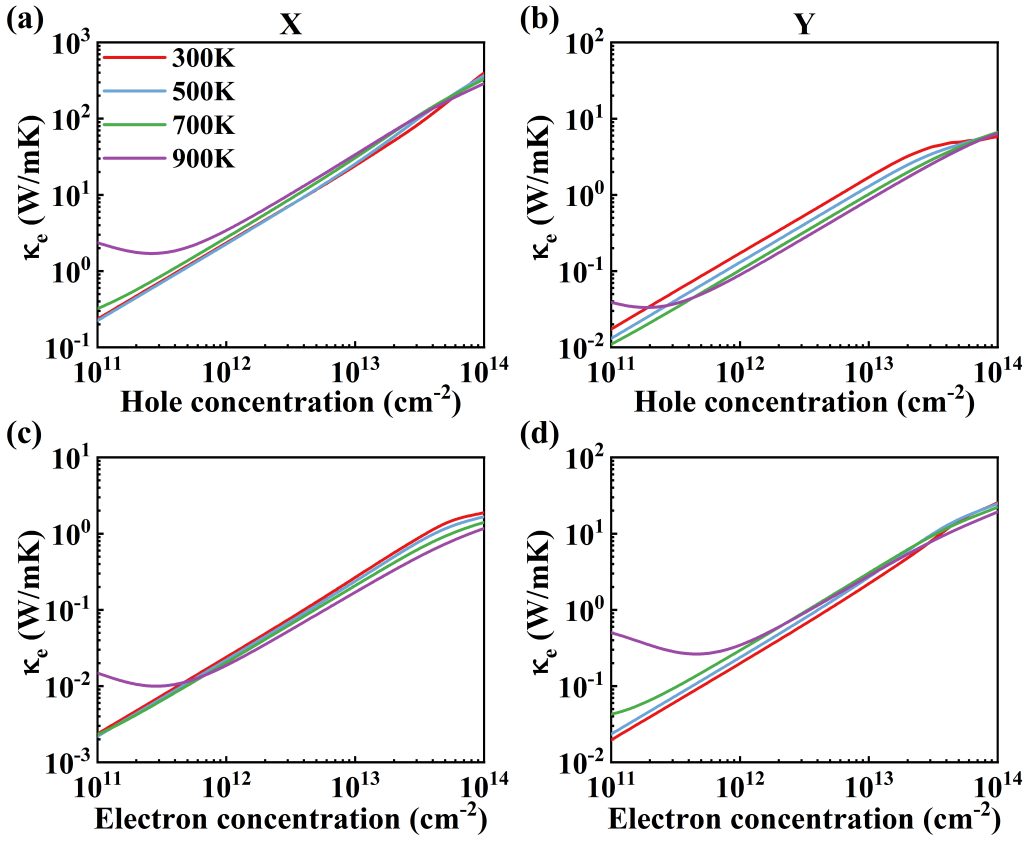

Fig. S11 The electronic thermal conductivity of the Mg_2Si monolayer as the function of (a, b) hole or (c, d) electron doping concentration along *x* or *y* direction at different temperatures at HSE06 method.

Table S1 Calculated equilibrium lattice parameters (a and b in Å), buckling distance (d in Å), bond length (Mg-Si in Å) and band gap (E_g in eV) of the 2D Mg_2Si monolayer.

Mg_2Si	a	b	d	<Mg-Si>1	<Mg-Si>2	<Mg-Si>3	<Mg-Si>4	E_g
our	7.319	4.363	2.036	2.672	2.690	2.670	2.681	0.51 (PBE)
								0.94 (HSE06)
other[6]	7.28	4.34	2.03					0.95 (HSE06)

Table S2 Calculated the elastic coefficient (C_{2D} in J/m^2), DP constant (E_1 in eV), effective mass (m^* in m_0), carrier mobility (μ in cm^2/Vs) and relaxation time (τ in fs) of 2D Mg_2Si at room temperature.

direction	carrier type	C_{2D}	E_1	m^*	μ	τ
x	electron	16.29	6.00	0.38	76.15	16.39
	hole	16.29	-0.38	0.59	15720.23	5298.82
y	electron	49.42	3.20	0.30	1029.36	174.65
	hole	49.42	-8.28	0.11	525.63	33.82

Table S3 Calculated Poisson's ratio and ZT of Mg_2Si monolayer and comparison materials. The ZT values represent their maximum at 300 K.

2D material	Poisson's ratio	ZT
Mg_2Si (this work)	-0.364	2.51
C_2H[7]	-0.071	0.93
C_2F[7]	-0.042	0.80
Ag_2S[8]	-0.11	0.72
AgCuS[8]	-0.06	0.84
pentagonal tellurene[9]	-0.01	2.84
Si_9C_{15}[10]	-0.175	1.25 (800 K)

References

1 E. Cadelano, P. L. Palla, S. Giordano and L. Colombo, *Phys. Rev. B*, 2010, **82**, 235414.

2 D. G. Cahill, S. K. Watson and R. O. Pohl, *Phys. Rev. B*, 1992, **46**, 6131.

3 Z. Gao, T. Zhu, K. Sun and J.-S. Wang, *ACS Appl. Electron. Mater.*, 2021, **3**, 1610-1620.

4 B. Y. Song, Y. Zhou, H. M. Yang, J. H. Liao, L. M. Yang, X. B. Yang and E. Ganz, *J. Am. Chem. Soc.*, 2019, **141**, 3630-3640.

5 F. Y. Li, X. D. Lv, J. X. Gu, K. X. Tu, J. Gong, P. Jin and Z. F. Chen, *Nanoscale*, 2020, **12**, 85-92.

6 A. Y. Alekseev, D. B. Migas, A. B. Filonov, V. E. Borisenko and N. V. Skorodumova, *Jpn. J. Appl. Phys.*, 2020, **59**, SF0801.

7 D. Singh, N. Khossossi, W. Luo, A. Ainane and R. Ahuja, *Mater. Today Adv.*, 2022, **14**, 100225.

8 W. Y. Fang, K. Kuang, H. R. Wei, X. L. Xiao, Y. Chen, M. K. Li and Y. B. He, *FlatChem*, 2022, **35**, 100416.

9 T. Zhang, J. H. Lin, X. L. Zhou and X. Jia, *Appl. Surf. Sci.*, 2021, **559**, 149851.

10 M. B. Tagani, *Phys. Rev. B*, 2023, **107**, 085114.